

## Highly conducting organic composites obtained by charge transfer reaction in the solid state

ANDRZEJ GRAJA\*, MYKOLA GOLUB

Institute of Molecular Physics, Polish Academy of Sciences, 60-179 Poznań, Poland

In this paper, we shortly present and discuss structural, electrical and spectral properties of organic composites with the general formulae  $(BEDT-TTF)_x/A$  and  $(BEDO-TTF)_x/A$ , where A denotes an electron-acceptor species such as iodine, AuI, or AuI<sub>3</sub>. Electron transfer between large conducting grains restricts electrical conductivity of the composites; the most probable mechanism being fluctuation-induced tunnelling conduction. Extensive spectral properties of organic composites are presented. It is shown that spectral studies can provide specific information about charge localization, electron-electron and electron-molecular vibration interactions, and about changes in the properties of highly conducting organic composites with ageing or annealing.

Key words: *organic composites; BEDT-TTF; BEDO-TTF; electrical transport; optical spectroscopy*

### 1. Introduction

Charge transfer (CT) complexes with the tetrathiafulvalene (TTF) organic donor or its derivatives possess very interesting physical properties such as high anisotropy and two-dimensional metal-like electron transport; some of them also show superconductivity and charge or spin ordering. However, these materials usually crystallize in the form of tiny and brittle crystals, which are difficult to handle and utilize. One of the possibilities of obtaining organic material in a form convenient for applications and with good physical properties is to prepare conducting organic composites directly in the solid state. As was shown by Brau and Farges [1, 2], charge-transfer reactions between suitable electron donor and acceptor moieties occur in the solid state in the course of grinding them together. Such a mechano-chemical method has been employed for the preparation of highly conducting composites of tetrathiafulvalene (TTF), *bis*(ethylenedithio)tetrathiafulvalene (BEDT-TTF), and *bis*(ethylenedioxy)tetrathiafulvalene (BEDO-TTF) [3–5], with various electron acceptors, e.g. iodine,

---

\* Corresponding author, e-mail: [graja@ifmpan.poznan.pl](mailto:graja@ifmpan.poznan.pl).

AuI, AuI<sub>3</sub>, and AuBr<sub>3</sub>. The main advantage of this method is an unlimited size and shape of the composite samples. Physical properties of such composites roughly resemble the properties of their crystalline analogues obtained by traditional ways. Grains forming the composite sample, however, are anisotropic and exhibit all the properties typical of single crystals. We have already widely exploited the method of Brau and Farges [1, 2], and some of our observations will be reviewed here.

## 2. Organic composites – preparation and structural properties

One of the methods of preparation of organic composites is to produce the conductive material by a CT reaction, which occurs directly in the solid state between organic electron donor and acceptor parent substances. The reaction is evidenced by a significant darkening of the mixture, prepared quite simply by crushing both donor and acceptor in an agate mortar. An appropriate molar proportion of substrates is ground for a defined time, then compacted and annealed (for details see [2–6]).

The morphology of the composites depends on their composition, and on the conditions of the synthesis and annealing procedure [7]. Usually, the morphology of the composite resembles the texture of a sponge. It has been suggested from X-ray diffractograms and Raman spectra that the composites are built mainly of grains, whose composition corresponds to the stoichiometry of the corresponding crystalline complexes, e.g. (BEDT-TTF)<sub>2</sub>I<sub>3</sub>, (BEDT-TTF)<sub>2</sub>AuI<sub>2</sub>, or (BEDO-TTF)<sub>2</sub>I<sub>3</sub> [8]. The conducting grains are separated by amorphous matter of various composition and electrical properties; in some cases, neutral grains of metallic gold also occur. This composition has been confirmed and described in detail by SEM imaging and energy dispersive X-ray analysis (EDX) [7, 9, 10]. From the SEM and EDX investigations, it was also stated that annealing the composite leads to the development and completion of the CT reaction, as well as to chemical exchange between components [5, 7, 9, 10].

## 3. Electrical transport properties – basic remarks

The electrical properties of BEDT-TTF- and BEDO-TTF-based composites have been recently reviewed [5, 11]; this is why the discussion of transport properties in this presentation will be limited to the most important problems.

BEDT-TTF-based composites exhibit a variety of electrical properties depending on their preparation conditions [5, 11, 12]. Samples of (BEDT-TTF)<sub>x</sub>/I, where  $x$  defines the molar proportions of solid donor and acceptor, show semiconducting behaviour before annealing. Appropriate thermal treatment, however, changes these properties from metal-like at high temperatures and semiconductor-like at low temperatures to metal-like behaviour over the entire temperature range (for properly annealed samples). Composites obtained by grinding BEDT-TTF with gold iodides (AuI or AuI<sub>3</sub>)

present similar properties, although in this case it is more difficult to obtain samples that display metallic conductivity in the whole temperature range [12].

The transport properties of BEDO-TTF-derived composites are completely different. The electrical conductivity of these materials reaches  $15 \text{ S}\cdot\text{cm}^{-1}$  at room temperature (RT) and is even higher when the temperature is lowered [4]. The prominent feature of  $(\text{BEDO-TTF})_x/\text{I}$  composites is their metal-like behaviour observed down to about 150 K for non-annealed samples (Fig. 1). On the other hand, ageing and annealing of BEDO-TTF composites causes the degradation of their transport properties.

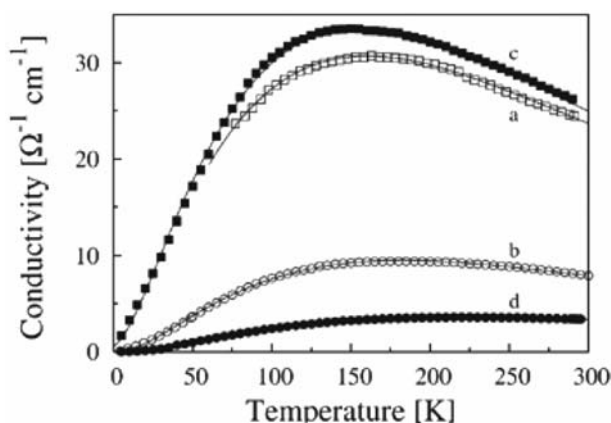


Fig. 1. Temperature dependence of the d.c. conductivity of: fresh (a) and 2-month (b) samples of  $(\text{BEDO-TTF})_{1.1}/\text{I}$  composite, a sample of  $(\text{BEDO-TTF})_{1.1}/\text{I}$  before (c) and after (d) annealing. Solid lines are fits with Eq. (1)

For the production of composites with desired electrical properties, it is very important to understand what mechanisms are responsible for temperature variations of the conductivity and to identify factors influencing electrical properties of the composites. Two mechanisms seem to be the most probable reasons for the semiconducting behaviour of non-annealed composite samples: charge carrier localization due to material defects and intergrain effects (poor contacts between grains). SEM investigations have shown that in BEDT-TTF-based composites during annealing both grain recrystallization and contact improvement between them take place. The first process can lead to a defect reduction and electron delocalization in grains, while the second improves the electrical transport between the grains. The crossover in annealed samples to semiconducting behaviour at low temperatures points out that one or both of the processes mentioned previously are not suppressed enough for metallic properties to be achieved at all temperatures.

From an analysis of the experimental data [13] it appears that fluctuation-induced tunnelling of the electrons (FIT) between grains is the most probable mechanism of composite conductivity at low temperatures [14]. Thermal fluctuations give rise to a decrease in intergrain resistances with increasing temperature, and the conductivity shows  $T^{-\alpha}$  behaviour typical of the contribution of metallic intragrain conductivity. To

fit experimental data at all temperatures, one can introduce the simplest model of the composite as a system of arrays with various resistances; one resistance represents the contribution of intergrain junctions and another one represents the grains themselves. In this case, the temperature dependence of composite conductivity can be approximated with the formula

$$\sigma(T) = \left[ B \exp\left(\frac{T_1}{T + T_0}\right) + CT^\alpha \right]^{-1} \quad (1)$$

where  $B$  and  $C$  are geometrical factors depending on the fraction of the sample length and cross-section area which correspond to the intergrain regions and conducting grains, respectively; the parameters  $T_0$  and  $T_1$  depend on the properties of contacts between grains [15]. The above equation can be fitted to experimental values of electrical conductivity. A good agreement between experimental data and fits allows one to suggest that the annealing of composites makes the influence of electron localization negligible and inhibits (but does not eliminate entirely) the undesirable effect of intergrain tunnelling. Using relations between  $T_0$ ,  $T_1$ , and the contact parameters (contact width, area, and barrier height) [15], one can find out, for example, how contact characteristics change with  $x$ , annealing conditions, grinding time, and other composite preparation parameters. This information is required to understand the processes of composite formation.

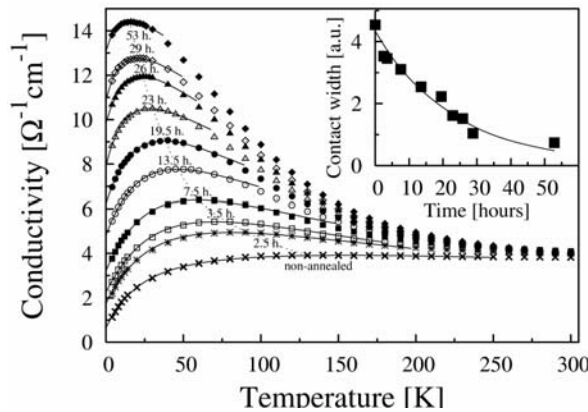


Fig. 2. Temperature dependence of the (BEDT-TTF)<sub>2.17</sub>/(AuI<sub>3</sub>) composite as a function of annealing time. Solid lines are fits by Eq. (1). In the insert, the changes of intergrain contact width on annealing, deduced from the fit parameters, are shown

The electrical properties of annealed BEDT-TTF composites almost do not change in time. On the other hand, the properties of non-annealed samples change with composite ageing [13]. Analysis of the experimental data shows that the ageing of non-annealed samples can be considered as non-effective annealing. The temperature de-

pendence of the conductivity of aged samples as a function of annealing time is shown in Fig. 2. Aged samples need to be annealed for tens of hours to achieve the same effect as fresh samples annealed for 1–2 hours. The conductivity of the (BEDT-TTF)<sub>2.17</sub>/(AuI<sub>3</sub>) composite has been analysed in terms of the FIT model in order to obtain information on how annealing influences intergrain contacts. The dependence of contact width on annealing time is shown in the insert of Fig. 2. Contact width decreases with annealing (contacts improve), which is in agreement with SEM observations.

An analysis of the temperature dependence of the conductivity of BEDO-TTF-derived composites (Fig. 1) shows that, as in the case of BEDT-TTF composites, the conductivity of these materials is determined mainly by two factors: 1) the metal-like conductivity of (BEDO-TTF)<sub>2.4</sub>I<sub>3</sub> grains and 2) fluctuation-induced tunnelling of carriers between grains. The  $T$ -dependence of BEDO-TTF composite conductivity can thus also be approximated by Eq. (1). As the conductivity of single crystals at high temperatures is proportional to  $T^{-2}$  [16], the parameter  $\alpha$  was taken to be equal 2.

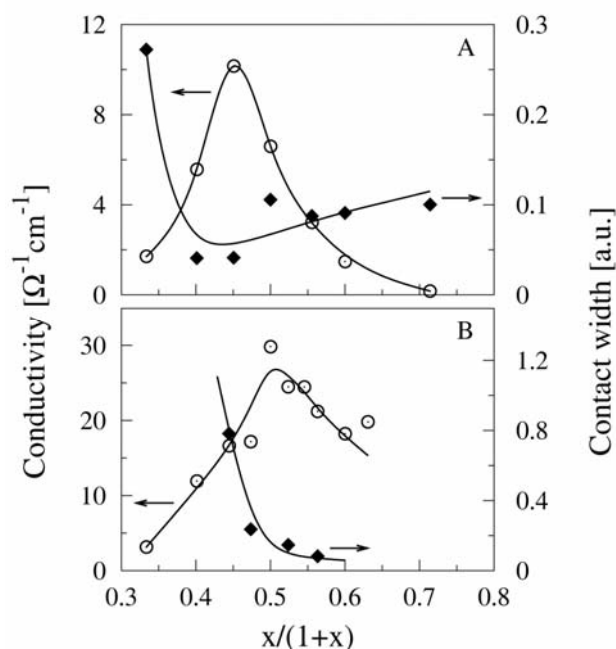


Fig. 3. Dependence of intergrain contacts on  $x$  for (BEDT-TTF) <sub>$x$</sub> /(AuI) (A) and (BEDO-TTF) <sub>$x$</sub> /I (B) composites. For comparison, the  $x$ -dependence of RT conductivity is presented. The solid curves are only to guide the eye

Changes in intergrain distances with  $x$  for (BEDO-TTF) <sub>$x$</sub> /I composites are shown in Fig. 3. Contrary to similar parameter variations for (BEDT-TTF) <sub>$x$</sub> /(AuI), no minimum of the contact width at  $x \approx x_{\text{opt}}$  is found in this case. These differences in the transport properties of both types of composites reflect the differences in their struc-

tures. In  $(\text{BEDT-TTF})_x/(\text{AuI})$ , conducting grains of  $(\text{BEDT-TTF})_2\text{I}_3$  and  $(\text{BEDT-TTF})_2\text{AuI}_2$  are formed. Grain concentration is the largest for  $x = x_{\text{opt}}$ , hence intergrain distance (contact width) is minimal. In  $(\text{BEDO-TTF})_x/\text{I}$ , an insulating phase of  $(\text{BEDO-TTF})\text{I}_3$  is formed together with conducting grains of  $(\text{BEDO-TTF})_2$ . This phase forms a layer between  $(\text{BEDO-TTF})_{2.4}\text{I}_3$  grains and unreacted iodine. The thickness of the  $(\text{BEDO-TTF})\text{I}_3$  shell decreases with increasing  $x$  due to the deficit of iodine, which also leads to a monotonic decrease in the contact width.

Suggestions resulting from analysing the temperature dependence of conductivity should be confirmed by other methods. IR investigations, discussed below, give additional information about conduction electrons and appear to be in agreement with the conclusions made here. Thermoelectric power measurements can also be used to confirm these suggestions [13, 17]. As shown by us, the same effect is observed for all types of annealed composites: although d.c. conductivity shows a strong  $x$ -dependence, the  $x$ -sensitivity of thermoelectric power is weak in the region of optimal composition ( $x_{\text{opt}}$ ) and above it. Not only RT thermoelectric power but also its temperature dependence do not depend on  $x$  when it is close to  $x_{\text{opt}}$  [13, 17]. In contrast to the conductivity, both thermoelectric power and its  $T$ -dependence change weakly with the annealing of composites for  $x \approx x_{\text{opt}}$ . Conducting microcrystals give the main contribution to the thermoelectric power of the composites [13, 17]. Weak sensitivity of the composites to thermal treatment means that the annealing influences mainly the non-conducting intergrain layers and weakly changes the thermoelectric properties of conducting grains. On the other hand, the thermoelectric properties of these microcrystals are almost the same as those of corresponding single crystals.

The interpretation of the electrical properties of BEDT-TTF and BEDO-TTF composites presented here allows one to make suggestions about ways to control and improve the electrical transport properties of composites obtained by direct CT reaction in the solid state. As intergrain conduction plays the most important role in BEDT-TTF composites, first of all one should try to improve the contacts between grains. One of the ways, proposed by us, is to apply the hot pressing method for organic composite production [13]. With this method, composites with better electrical transport characteristics have been obtained. Better intergrain contacts in composites prepared by hot pressing are responsible for improvement in their electrical properties. In BEDO-TTF-derived composites, mainly the insulating  $(\text{BEDO-TTF})\text{I}_3$  shell affects the electrical properties of the composites and their changes on ageing. Therefore, to improve the transport properties and stability of composites one should suppress  $(\text{BEDO-TTF})\text{I}_3$  phase formation or use some procedure to remove this phase after the composite has been prepared.

#### 4. Spectral properties of organic composites

Optical spectral studies play an important role in the investigation of organic conductors, including not only crystalline but also polymeric and other unconventional

forms, such as highly conducting organic composites obtained by direct CT reaction in the solid state. Properties of organic conductors are determined by various interactions and instabilities. The optical properties of these materials can be roughly described by the simplest model, assuming non-interacting electrons (the one-electron model). In this approximation, the infrared (IR) properties may be derived in the self-consistent approximation. Assuming a frequency-independent relaxation rate  $\gamma$  and a background electric permeability  $\varepsilon_0$  arising from high-frequency transitions, the result takes the Drude form [18]:

$$\varepsilon^*(\omega) = \varepsilon_0 - \frac{\omega_p^2}{\omega^2 - i\omega\gamma} \quad (2)$$

where  $\omega_p$  is the plasma frequency. This expression is frequently used to describe the optical properties of organic metal-like conductors in the IR region and to estimate some of their electron parameters. On the other hand, electron-molecular vibration (e-mv) coupling plays a fundamental role in organic conductors. In general, the interaction of electrons with intramolecular vibrations can be written in the form given by Rice [19]:

$$H = H_e + H_v + \sum_{\alpha,i} g_{\alpha} n_i Q_{\alpha i} \quad (3)$$

The first two terms describe radical electrons and molecular vibrations in the absence of vibronic coupling. A linear e-mv coupling is expressed explicitly by the third term. The set  $\{g_{\alpha}\}$  of constants denotes linear  $\pi$ -electron-molecular vibration constants.

Vibrational spectroscopy plays an important role in the characterization of highly conducting organic composites. Major spectroscopic interest is centred in the following areas: 1) differentiation and identification of various phases in composites and the evaluation of the charge distribution on their grains; 2) determining the extent of charge transfer from a donor to an acceptor moiety as a result of the CT reaction in the solid state; 3) determining of optical anisotropy, electronic structure, plasma frequencies, optical band gap, optical conductivity, and other parameters characterising electronic properties of the composite grains; 4) evaluating surface homogeneity of composite samples; 5) assignment of vibrational features. As will be shown below, the data mentioned above are helpful in offering a model of composite structure.

It is known from SEM and EDX investigations [7, 9, 10] that composites obtained by CT reaction in the solid state have a complex heterogeneous structure, containing grains of various compositions and properties, as well as intergrain matter. These observations of composite morphology, however, cannot give more exact information, maybe beyond confirming the existence of free gold grains in BEDT-TTF composites with gold iodides. As a microscopic tool, vibrational spectroscopy can differentiate between grains that exhibit metallic conductivity, e.g. (BEDT-TTF)<sub>2</sub>I<sub>3</sub>, (BEDT-TTF)<sub>2</sub>AuI<sub>2</sub>, and (BEDO-TTF)<sub>2.4</sub>I<sub>3</sub>, and those that are semiconducting or insulating.

The IR spectra of the complexes show characteristic features, such as interband transitions (usually in the range of  $1000\text{--}4000\text{ cm}^{-1}$ ), accompanied by very strong and broad vibronic bands originating from a coupling of electronic excitations with the totally symmetric ( $A_g$ ) intramolecular vibrations of the organic donor molecules (such as BEDT-TTF or BEDO-TTF). The latter features are localized between  $100$  and  $1500\text{ cm}^{-1}$ , with a characteristic strong absorption near  $1250\text{ cm}^{-1}$  [20]. The spectra of semiconducting composites, complexes, or ion-radical salts show distinct CT bands with an onset between  $1500$  and  $2500\text{ cm}^{-1}$  and a well developed set of vibronic bands corresponding to  $A_g$  modes of the donor molecule. The spectra of metal-like composites or other organic conductors are, oppositely, dominated by the broad and strong absorption given by conduction electrons. The strongest vibronic band or bands are usually detectable as sub-maxima on the broad electronic absorption [20]. Such qualitative information can be restated precisely by Raman scattering investigations.

Raman scattering spectra of selected BEDT-TTF-derived composites, namely  $(\text{BEDT-TTF})_{0.67}/\text{I}$ ,  $(\text{BEDT-TTF})_2/\text{AuI}_3$ , and  $(\text{BEDT-TTF})_{0.82}/\text{I}$ , are shown in Fig. 4 [8]. The maximum at  $30\text{ cm}^{-1}$  is attributed to bending and the one at  $120\text{ cm}^{-1}$  to stretching vibrations of the  $\text{I}_3^-$  anion. In the spectra of  $(\text{BEDT-TTF})_2/\text{AuI}_3$  and  $(\text{BEDT-TTF})_{0.82}/\text{I}$ , one can also see the  $\text{I}_3^-$  line, and an additional band at  $160\text{ cm}^{-1}$ , which can be assigned to stretching vibration of the  $\text{AuI}_2^-$  anion [21]. This suggests that there are also  $(\text{BEDT-TTF})_2\text{AuI}_2$  grains in the two latter composites, except in  $(\text{BEDT-TTF})_2\text{I}_3$ . This is corroborated by an analysis of the range  $20\text{--}60\text{ cm}^{-1}$ , corresponding to bending vibrations, where a distinct evolution with the appearance of a new band below  $60\text{ cm}^{-1}$  is observed.

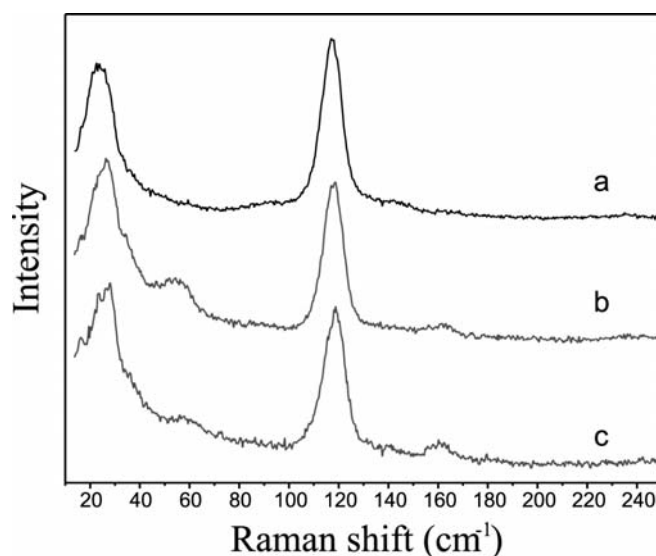


Fig. 4. Resonant Raman scattering spectra of  $(\text{BEDT-TTF})_{0.67}/\text{I}$  (a),  $(\text{BEDT-TTF})_{0.82}/\text{AuI}$  (b), and  $(\text{BEDT-TTF})_2/\text{AuI}_3$  (c) composites



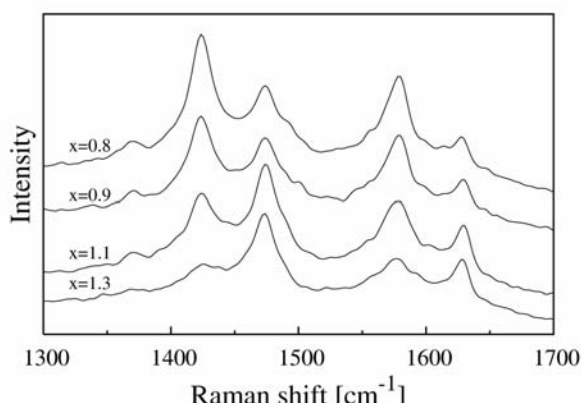


Fig. 5. Raman spectra of  $(\text{BEDO-TTF})_x/\text{I}$  composites in the frequency range of C=C stretching vibrations

Phase identification and evaluation of charge on the donor moieties can be performed with IR or Raman spectroscopy. The latter is more accurate, since Raman lines are better separated than IR bands. Raman spectra of  $(\text{BEDO-TTF})_x/\text{I}$  composites in the most interesting range, between 1300 and 1700  $\text{cm}^{-1}$ , are shown in Fig. 5. These spectra, independent of sample composition (described by the parameter  $x$ ), consist of four lines at 1424, 1474, 1578, and 1630  $\text{cm}^{-1}$ . These lines are assigned to  $A_g$  stretching vibrations of the central and ring C=C bonds, respectively, downshifted according to the value of charge on the BEDO-TTF cations in the composites [22, 23]. A similar effect, a linear correlation between vibrational band localization and charge on the considered bond has been observed some time ago by Farges et al. [1] in their studies on the IR absorption of the  $\text{TEA}(\text{TCNQ})_2$  organic conductor. The presence of four lines in the Raman spectra of  $(\text{BEDO-TTF})_x/\text{I}$  composites suggests that two kinds of microstructures (grains) co-exist in the composites [24]. The doublet at 1474 and 1630  $\text{cm}^{-1}$  is characteristic of one grain type and the doublet at 1424 and 1578  $\text{cm}^{-1}$  of the other. Ionisation shifts are approximately 53 and 27  $\text{cm}^{-1}$  in the former case, and 104 and 79  $\text{cm}^{-1}$  in the latter case [25]. In order to evaluate the CT degree ( $\rho$ ) on the cation, a linear dependence between the frequencies of the two totally symmetric C=C modes and the charge on the BEDO-TTF was assumed. Using the formulae of Drozdova et al. [23]:

$$\rho = \frac{1524.9 - \nu_{3,\text{obs}}}{109.0}, \quad \rho = \frac{1660.8 - \nu_{2,\text{obs}}}{74.1} \quad (4)$$

where  $\nu_{3,\text{obs}}$  and  $\nu_{2,\text{obs}}$  are the observed wave numbers of the bands, one can evaluate the degrees  $\rho' = 0.42$  and  $\rho'' = 1.0$  of each expected microstructure type for  $(\text{BEDO-TTF})_x/\text{I}$  composites [24, 25]. The former one corresponds to the crystal stoichiometry of 2.4:3 and the latter to 1:3. This indicates that the composite contains two phases,  $(\text{BEDO-TTF})_{2.4}\text{I}_3$  and  $(\text{BEDO-TTF})\text{I}_3$ .

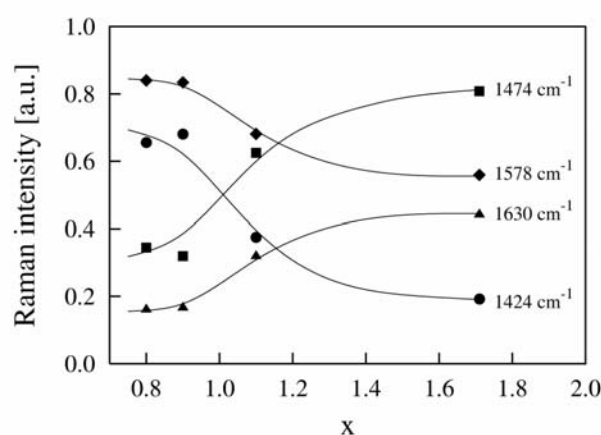


Fig. 6. Raman intensity of the C=C Raman lines as a function of  $x$  for (BEDO-TTF) $_x$ /I composites. The solid curves are only to guide the eye

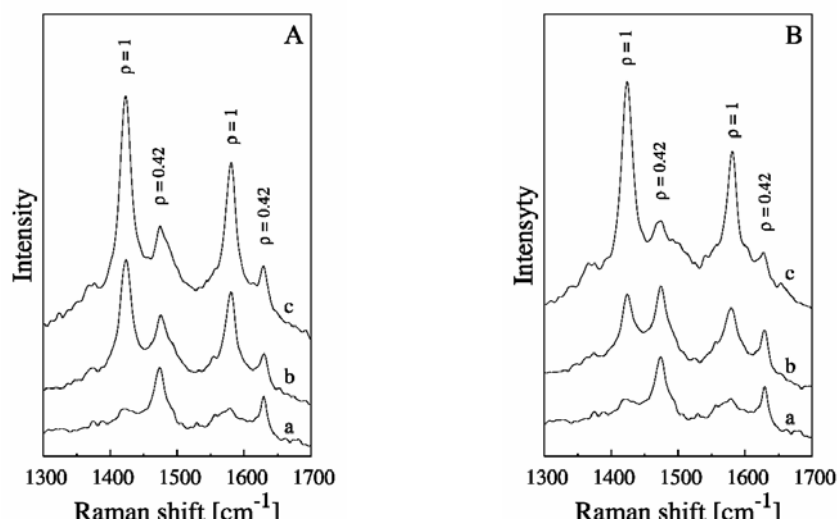


Fig. 7. Raman spectra of (BEDO-TTF) $_{1.0}$ /I composites: A) spectra of : 9- (a), 15- (b), and 38- (c) day old samples; B) spectra of non-annealed (a) and annealed (b, c) samples; the latter were annealed for 1 h (b) and 2 h (c) at a temperature of 80° C

The contents of grains of both types strongly depend on the sample composition (Fig. 6), its age, and thermal treatment (Fig. 7) [25]. The intensity of Raman lines (Fig. 6), characteristic of (BEDO-TTF) $_{2.4}$ I $_3$ , decreases in the region of optimal composition ( $x \approx 1$ ). The intensity of the lines assigned to (BEDO-TTF)I $_3$ , however, increases in the same region. This means that for  $x < 1$  and  $x > 1$  the relative amounts of (BEDO-TTF)I $_3$  and (BEDO-TTF) $_{2.4}$ I $_3$  phase are different. The ageing process for the (BEDO-TTF) $_{1.0}$ /I composite is illustrated in Fig. 7A. The Raman spectrum of a relatively fresh sample is dominated by the lines at 1474 and 1630  $\text{cm}^{-1}$ . These compo-

nents decrease slightly during the ageing of the sample; at the same time, the components at 1424 and 1578  $\text{cm}^{-1}$  increase distinctly and become dominant after about 40 days. This evolution shows that the phase with the stoichiometry of 2.4:3 dominates in the beginning, but during ageing the contents of the 1:3 phase prevails. This process can be enhanced if the sample is annealed, as is shown in Fig. 7B. These spectral results show that annealing causes an evolution of the sample towards increased content of the (BEDO-TTF) $\text{I}_3$  phase. This is a low-conducting phase, therefore the electrical conductivity of the BEDO-TTF composite decreases strongly with annealing.

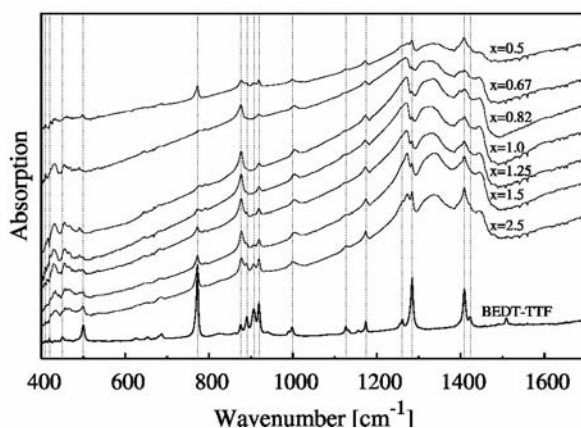


Fig. 8. Absorption spectra of  $(\text{BEDT-TTF})_x/(\text{AuI})$  composites for various sample compositions, recorded in a KBr matrix; the spectrum of neutral BEDT-TTF, taken in the same conditions, is shown for comparison

The IR spectra of the composites also give important information on the samples [20, 24–28]. Absorption spectra of  $(\text{BEDT-TTF})_x/(\text{AuI})$  composites in the most interesting spectral region, for various sample compositions, recorded in a KBr matrix, are shown in Fig. 8. For comparison, the spectrum of neutral BEDT-TTF, taken in the same conditions, is also shown. The spectra are typical of conducting BEDT-TTF materials [3, 26, 27] and are similar to those of BEDO-TTF composites [24, 25]. They can be roughly divided into two parts: 1) from 7000  $\text{cm}^{-1}$  to the sharp absorption increase at about 1600  $\text{cm}^{-1}$  (not shown here) and 2) from 1600 to 600  $\text{cm}^{-1}$ . In the first part, quite a broad absorption band is observed with a maximum between 3200 and 2900  $\text{cm}^{-1}$ , depending on the sample composition. This band is generally assigned to an electronic interband transition between split bands. The splitting is caused by strong intermolecular interactions between electron donor and acceptor molecules. This feature can be viewed as the plasma part of the spectrum. The second, most informative part of the IR spectra of the composites, shows a very rich vibrational structure. The majority of the observed bands can be assigned to the normal vibrations of  $\text{BEDT-TTF}^+$  (or  $\text{BEDO-TTF}^+$ ) cations. These bands are down-shifted with respect to the corresponding bands of the neutral donor. The shifts are independent of the

sample molar composition and are influenced by the average electron charge on the donor and by a modified charge distribution on the donor moieties after composite formation. A broadening of these bands is observed with increasing donor concentration in the mixture, which is characteristic of the formation of highly conducting composites as well as crystalline complexes [3, 25–27]. There are two particularly interesting bands in the IR spectra of BEDT-TTF and BEDO-TTF composites: in BEDT-TTF composites, a broad band centred at about  $1320\text{ cm}^{-1}$  and a structure at about  $1400\text{ cm}^{-1}$ , and in BEDO-TTF-derived materials at about  $1340\text{ cm}^{-1}$  and  $1600\text{ cm}^{-1}$ . The coupling of totally symmetric normal vibrations ( $A_g$  modes) in a donor molecule with appropriate electronic excitations [27, 28] is the origin of the activation of these bands. The  $A_g$  modes mentioned above are attributed to the stretching of the central and ring C=C bonds, respectively [22, 27].

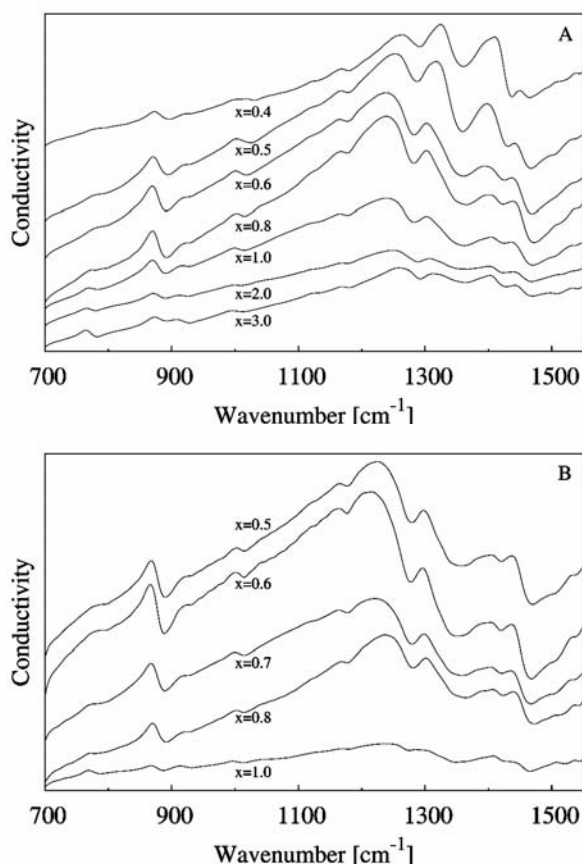


Fig. 9. Optical conductivity spectra of  $(\text{BEDT-TTF})_x\text{I}$  composites before (A) and after (B) annealing, for various  $x$ , recorded in a KBr matrix

As was shown before, BEDT-TTF composite conductivity, which is semiconductor-like just after preparation (before annealing), becomes metallic after appropriate

thermal treatment. Such a drastic change in physical properties can also be observed by IR spectral methods. For example, the optical conductivity spectra, which are equivalent to absorption spectra of  $(\text{BEDT-TTF})_x\text{I}$  composites before and after annealing, for various  $x$ , are shown in Fig. 9. After annealing, the bands become broader, are down-shifted and overlap with the broad and strong electronic absorption caused by conducting electrons. The conducting electrons are responsible for plasma-edge-like dispersion, which appears in the near IR region both for highly conducting crystalline synthetic metals and for metal-like organic composites. The IR reflectivity spectrum of the  $(\text{BEDO-TTF})_{1.0}\text{I}$  composite and a least-square fit to the reflectance calculated from the Drude model [18] (dashed line) are shown as an example in Fig. 10. From the best fit one can evaluate fitting parameters such as  $\omega_p$ ,  $\gamma$ ,  $\epsilon_0$ , relaxation time  $\tau$ , mean free path of charge carriers  $\lambda$ , and optical conductivity at zero frequency  $\sigma_{\text{opt}}(0)$ . It is difficult to directly compare such evaluated transport parameters with the parameters for corresponding crystalline complexes due to their anisotropy and to the scattering of data from various papers, even for the same material. The plasma frequency and dielectric constant evaluated for composites are usually reasonable when compared with data for related single crystals, but the damping rate of the composites is significantly higher than that of single crystals with the same composition [24]. The transport of charge carriers is strongly damped in composites due to their granular structure and grain defects. Consequently, the mean free path is relatively short.

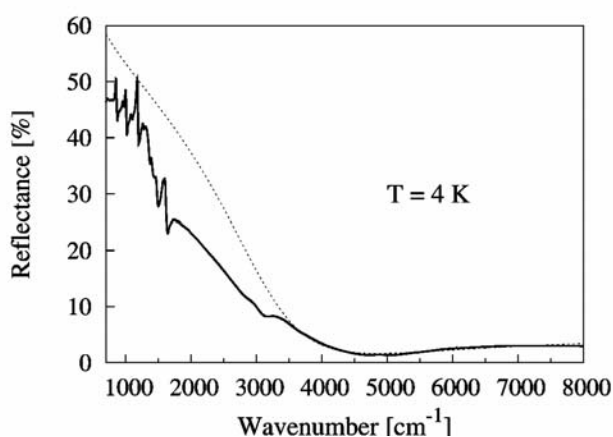


Fig. 10. Reflectance spectrum of the  $(\text{BEDO-TTF})_{1.0}\text{I}$  composite. Least-square fit to the reflectance, calculated from the Drude model, is shown by the dashed line

Microreflectance studies of composites suggest that the organic conductors obtained by CT reaction in the solid state are macroscopically homogeneous [26, 27]. This observation is conformable to SEM and EDX investigations. Besides, spectral methods are appropriate for characterizing materials and confirming the appearance of particular molecular groups. Various IR spectral methods (absorption of composites

dispersed in KBr pellets, absorption of very thin composite samples, reflectance from the composite surface, optical conductivity evaluated from composite reflectance), supplemented by Raman scattering studies, give extensive information on the spectral properties of the investigated materials.

As mentioned in this chapter, optical studies of organic composites are crucial for understanding their macroscopic structure, electronic interactions, and electronic structure. Information comes from studies in the wide spectral region, from far IR to vacuum ultraviolet. Spectral studies of organic composites can provide specific information about the localization of charges, electron-electron and electron-molecular vibration interactions, vibronic activations of the modes, phase transitions, and changes in the properties of highly conducting organic composites with ageing or annealing.

## 5. Concluding remarks

The synthesis of non-traditional organic materials that display good physical properties, in particular high electrical conductivity, optical transparency or nonlinearity, and good stability, is an important aspect of contemporary molecular engineering. Organic conductors are precursors of such momentous species as nano-materials. At present, it is possible to fabricate various organic conductors not only as crystals but also in the form of thin conducting films, conducting reticulate doped polymeric films, or polycrystalline samples. Although these materials are of great practical importance, they exhibit some shortcomings. One of them is the rather difficult and expensive technology associated with them. This is why we present a relatively simple mechano-chemical way of preparing conducting organic composites.

We have given a discussion of the basic problems concerning the physical properties of BEDT-TTF- and BEDO-TTF-derived composites, especially their spectral properties. It seems that a better understanding and description of the phenomena occurring in these type of new organic materials are necessary to both develop their technology and to discover their applications in molecular electronic devices.

### Acknowledgement

The authors are grateful to Dr. Iwona Olejniczak for her critical reading of the manuscript.

### References

- [1] FARGES J.P., BRAU A., DUPUIS P., *Solid State Commun.*, 54 (1985), 531.
- [2] FARGES J.P., BRAU A., [in:] H.S. Nalwa (Ed.), *Handbook of Advanced Electronic and Photonic Materials and Devices*, Academic Press, San Diego, 2001, p. 329–369.
- [3] SEMKIN V.N., GRAJA A., SMIRANI I., BRAU A., FARGES J.P., *J. Mol. Struct.*, 511/512 (1999), 49.
- [4] GRAJA A., BRAU A., FARGES J.P., *Synth. Met.*, 122 (2001), 233.
- [5] GRAJA A., GOLUB M., *Compt. Rend. Chimie*, 6 (2003), 367.

- [6] BRAU A., SMIRANI I., FARGES J.P., LIPIEC R., GRAJA A., *Synth. Met.*, 108 (2000), 75.
- [7] GOLUB M., SZCZEŚNIAK L., GRAJA A., BRAU A., FARGES J.P., *J. Mater. Sci.*, 36 (2001), 5543.
- [8] GRAJA A., BRAU A., FARGES J.P., GOLUB M., TRACZ A., JESZKA J.K., *Synth. Met.*, 120 (2001), 753.
- [9] GOLUB M., GRAJA A., BRAU A., FARGES J.P., *Synth. Met.*, 125 (2002), 337.
- [10] GOLUB M., GRAJA A., JÓŹWIAK K., *Synth. Met.*, 144 (2004), 201.
- [11] GRAJA A., GOLUB M., *Nonlinear Optics Quantum Optics*, 32 (2004), 21.
- [12] GOLUB M., GRAJA A., BRAU A., FARGES J.P., *Synth. Met.*, 125 (2002), 301.
- [13] GOLUB M., Ph.D. Thesis, Institute of Molecular Physics, Polish Academy of Sciences, Poznań, 2003.
- [14] SHENG P., *Phys. Rev. B*, 21 (1980), 2180.
- [15] PAASCH G., LEHMANN G., WUCKEL L., *Synth. Met.*, 37 (1990), 23.
- [16] WUDL F., YAMACHI H., SUZUKI T., ISOTALO H., FITE C., KASMAI H., LIOU K., SRDANOV G., *J. Am. Chem. Soc.*, 112 (1990), 2461.
- [17] GOLUB M., GRAJA A., *J. Physics D: Appl. Phys.*, 36 (2003), 3064.
- [18] BORN M., WOLF E., *Principles of Optics*, Pergamon Press, New York, 1959.
- [19] RICE M.J., *Solid State Commun.*, 31 (1979), 93.
- [20] GRAJA A., *Low-Dimensional Organic Conductors*, World Scientific, Singapore, 1992.
- [21] OHTSUKA I., NAKAYAMA H., ISHI. K., *J. Raman Spectr.*, 20 (1989), 489.
- [22] POKHODNIA K.I., KOZLOV M.E., ONISCHENKO V.G., SCHWEITZER D., MOLDENHAUER J., ZAMBONI R., *Synth. Met.*, 56 (1993), 2364.
- [23] DROZDOVA O., YAMACHI H., YAKUSHI K., URUICHI M., HORIUCHI S., SAITO G., *J. Am. Chem. Soc.*, 122 (2000), 4436.
- [24] GRAJA A., ŚWIETLIK R., POŁOMSKA M., BRAU A., FARGES J.P., *Synth. Met.*, 125 (2002), 319.
- [25] GOLUB M., GRAJA A., POŁOMSKA M., *phys. status solidi (a)*, 194 (2002), 226.
- [26] SMIRANI I., SEMKIN V.N., GRAJA A., BRAU A., FARGES J.-P., *Synth. Met.*, 102 (1999), 1263.
- [27] GRAJA A., *Optical properties* [in:] J.-P. Farges (Ed.), *Organic Conductors*, Marcel Dekker, Inc., New York, 1994, p. 229.
- [28] RICE M.J., LIPARI N.O., STRÄSSLER S., *Phys. Rev. Lett.*, 39 (1977), 1359.

Received 14 September 2004

Revised 29 October 2004